IMPACT OF SIMULTANEOUS OPERATION OF AIR CONDITIONERS ON POWER SYSTEMS

Sergio M. R. Sanhueza, Geraldo C. Guimarães, José C. Oliveira, Carlos G. Medeiros
Bismarck C. Carvalho, Fernando L. Tofoli, Fábio L. Albuquerque
Universidade Federal de Uberlândia – Faculdade de Engenharia Elétrica
Av. João Naves de Ávila, 2160, Campus Santa Mônica, Bloco "3N"
CEP 38400-902, Uberlândia, MG, Brasil, +55-34-32394166
E-mail: sergiorivera@pop.com.br

***Abstract* – The intense and widespread use of air conditioners have caused the reactive power demand of the grid system to increase. Therefore, the presence of such type of load deserves special attention, since the power system may collapse when submitted to overload and voltage sags. Such phenomena are used in this paper in order to establish a comparison between computational and experimental results obtained when a room air conditioner is employed. Four mathematical models are proposed and tested for this device.**

KEYWORDS

Load modeling, air conditioners, voltage sag, frequency variation, power quality.

I. INTRODUCTION

The choice of an adequate modeling for a single load, or even a group of loads, in power systems can have great influence on the results and conclusions obtained in stability and load shedding studies. An inaccurate modeling may provide conclusions that compromise the system operation, such as inadequate reactive power compensation, insufficient reactive power reserve specification and bad emergency decisions.

Within this context, air conditioner loads deserve special attention, since they correspond to a significant part of the system load, i.e., it means up to 25% of the power demand in the residential sector. This type of load generally uses asymmetrical two-phase induction motors, which are composed by two windings, as shown in Figure I, i.e., a main winding, responsible for the steady state operation and an auxiliary winding, responsible for the motor startup.

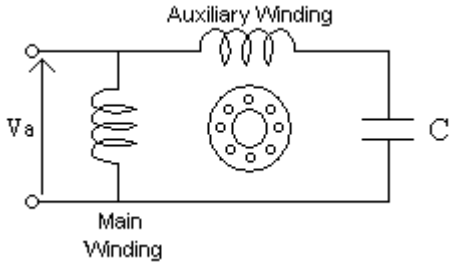

FIGURE I
Motor arrangement used in window type air conditioners

Capacitor "C", in Figure I, is necessary for the startup and power factor correction in steady state operation. Since the capacitor is designed to operate at the motor full speed, the startup conjugate is reduced [1].

Thus, the system may not reaccelerate the motor after the occurrences of voltage sags, because the power factor is low and high currents cause significant voltage drops on the feeders. In many cases, the voltage could not be reestablished, causing the system to collapse [2] [3] [4].

Considering all these facts, this paper aims to investigate the performance of an air conditioner load when voltage sags and frequency variation occur in the power system.

II. AIR CONDITIONERS REPRESENTATION

Four mathematical and computational models are evaluated for room air conditioners, as shown in Table I. The studies performed aim to verify the active and reactive power responses against voltage and frequency variations applied to the equipment.

The simplest model employs constant power, since this can represent the behavior of the induction motor for ideal conditions of voltage and frequency. The second and third representations consist in the polynomial and exponential models, respectively, developed by EPRI (Electric Power Research Institute) [5], which consider not only the effects of the voltage variation, but also the influence of the frequency. The fourth model is formulated in the time domain, where the asymmetrical two-phase induction motor is represented by algebraic and differential equations.

TABLE I
Characteristics of the models analyzed

Model	Description	Domain
1	Constant power	Frequency
2	Polynomial	Frequency
3	Exponential	Frequency
4	Dynamic	Time

The first three static models are easily found in technical publication [5] and will not be considered any further. Due to its importance, the dynamic modeling of room air conditioners will be detailed in the next section.

III. AIR CONDITIONER DYNAMIC MODELING

In order to represent mathematically the motor, it is necessary to deal with stator and rotor circuits separately, as indicated in Figure II. The stator is composed by two windings, whose axes are 90° phase shifted: a main winding and an auxiliary winding in series with a capacitor "C". Similarly, the rotor is also represented by two identical short-circuited windings, whose axes are also 90° phase shifted.

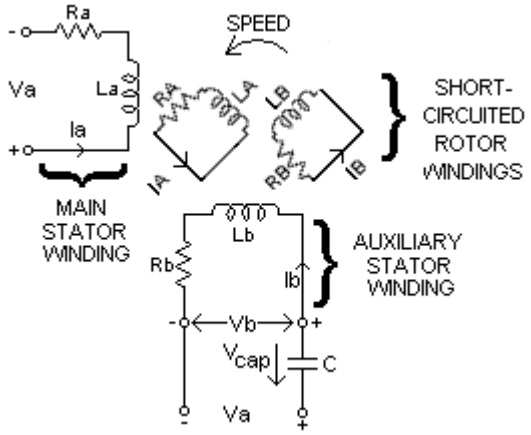

FIGURE II
Equivalent circuits concerning the phase windings.

III.1 Electrical equations

Voltage expressions corresponding to stator and rotor circuits can be obtained to describe the motor behavior. Stator equations are given in (1) and (2):

$$v_a = r_a i_a + \frac{d\lambda_a}{dt} \quad (1)$$

$$v_b = r_b i_b + \frac{d\lambda_b}{dt} \quad (2)$$

where subscripts a, b represent the phases a and b of the stator windings, respectively, and:

- v = instantaneous voltage;
- r = resistance,
- i = current;
- λ_i = flux linkage;
- t = time.

Since the rotor windings are short circuited, the following expressions are valid:

$$r_A i_A + \frac{d\lambda_A}{dt} = 0 \quad (3)$$

$$r_B i_B + \frac{d\lambda_B}{dt} = 0 \quad (4)$$

where subscripts A and B represent the rotor windings in phases A and B, respectively.

The capacitor current can be written in function of its voltage (v_{cap}) and capacitance (C) as.

$$i_b = C\frac{dv_{cap}}{dt} \quad (5)$$

According to Figure II, equation (1) and (2) are related by:

$$v_a = v_{cap} + v_b \quad (6)$$

III.II Mechanical equation

The instantaneous electromagnetical torque can be derived from the magnetic co-energy variation in relation to the rotor angle displacement, considering the currents fixed. This is represented in (7). Then, by determing the co-energy variation, equations (7) and (8) can be used to provide the electromagnetical torque, which results in (9).

$$T = \frac{\partial W'_m}{\partial \theta_{mec}} \quad (7)$$

$$\theta_e = \frac{p}{2}\theta_{mec} \quad (8)$$

$$T = \frac{p}{2}\sum_i\sum_j i_i i_j \frac{dL_{ij}}{d\theta_e} \quad (9)$$

Notation used in equations (7) to (9):
W'_m= co-energy variation;
θ_{mec}= rotor mechanical angle;
θ_e = rotor electrical angle;
p = number of poles;
i = winding current;
L_{ij} = mutual inductance between windings i and j;
i = subscripts a and b, for stator phases a and b;
j = subscripts A and B, for rotor phases A and B.

III.III Dynamic equations

According to the assumptions presented above, the following expressions can be written to relate the flux linkages with the self and mutual inductances between the windings:

$$\lambda_a = L_{aa} i_a + L_{aA} i_A + L_{aB} i_B \quad (10)$$

$$\lambda_b = L_{bb} i_b + L_{bA} i_A + L_{bB} i_B \quad (11)$$

$$\lambda_A = L_{AA} i_A + L_{Aa} i_a + L_{Ab} i_b \quad (12)$$

$$\lambda_B = L_{BB} i_B + L_{Ba} i_a + L_{Bb} i_b \quad (13)$$

The mutual inductances between windings "i" and "j" are:

$$L_{aA} = M_{aA}\cos\theta_e = L_{Aa} \quad (14)$$

$$L_{aB} = M_{aB}\cos(\theta_e - 90^o) = M_{aB}\,\mathrm{sen}\,\theta_e = L_{Ba} \quad (15)$$

$$L_{bA} = M_{bA}\cos(\theta_e + 90^o) = -M_{bA}\,\mathrm{sen}\,\theta_e = L_{Ab} \quad (16)$$

$$L_{bB} = M_{bB}\cos\theta_e = L_{Bb} \quad (17)$$

$$L_{ab} = M_{ab}\cos 90^o = L_{ba} = 0 \quad (18)$$

$$L_{AB} = M_{AB}\cos 90^{o} = L_{BA} = 0 \qquad (19)$$

III. EXPERIMENTAL ARRANGEMENT AND DATA

Experimental tests have been carried out using a special programmable power supply, HP 6834A, which provides the control of the amplitude and frequency of the supply voltage waveform. A digital oscilloscope connected to a PC has also been employed to acquire data. The experimental arrangement is shown in Figure III.

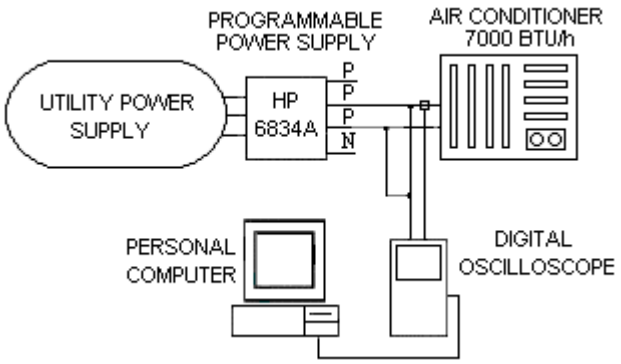

FIGURE III
Experimental arrangement

The air conditioner used in the test has rated power and voltage equal to 950 W (7000 BTU/h) and 220 V, respectively. It is also important to mention that the air conditioner uses a small fan that cools the condenser and also injects cold air in the environment. It requires 0.6 A current, approximately, as it operates continuously. Such current was measured experimentally, along with that required by the compressor, and this value is greater than that obtained via simulation, where the fan was not considered.

IV. RESULTS AND ANALYSES

In order to analyze the models presented previously [5] [6], the simulating package SABER [7] was used. To make simpler the analysis, per-unit (pu) values are adopted, using 950 W and 220 V, respectively, as reference (base) values for power and voltage.

The analyses seeks to verify the behavior of the active and reactive powers in function of voltage and frequency variation. The three cases studies, described in Table II, are common disturbances that may occur on power systems.

TABLE II
Case studies

Case	Description
1	Voltage Sag: 10% during 10 cycles
2	Voltage Sag: 30% during 05 cycles
3	Frequency variation between 57 and 63 Hz for voltages equal to 0.9, 1.0 and 1.1 pu

The parameters of equivalent circuits shown in Figure II employed in the experimental test are provided in Table III.

TABLE III
Parameters

Parameter	Value
Ra	3.86ohms
Xa	5.44 ohms
Rb	11.49 ohms
Xb	3.44 ohms
RA	4.5 ohms
XA	2.5 ohms
RB	4.5 ohms
XB	2.5 ohms
C	17.5μF
J	0.0015kgm^2

To facilitate the analysis, all graphics are plotted using the same scale for experimental and simulation results.

V.1 Case 1: 10% Voltage Sag during 10 cycles

The voltage is decreased from 1.0 to 0.9 pu and kept in this value during 10 cycles, applied to the room air conditioner. The active power and the reactive power measurements, together with the voltage disturbance, are shown in Figure IV.

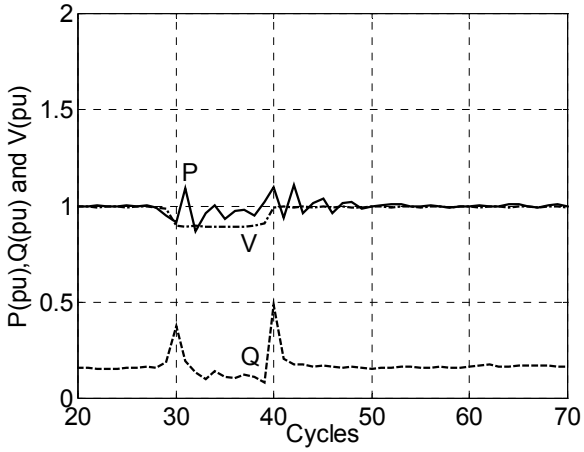

FIGURE IV
Voltage applied and active and reactive powers responses (case 1 experimental results)

The active power is firstly reduced along the voltage sag and then it oscillates, trying to go back to its rated value. Just after the end of the voltage sag, the active power increases suddenly and becomes oscillatory for around 10 cycles.

The reactive power is even more troublesome, since it reaches 0.35 pu (about twice the nominal value, 0.17 pu) when the voltage sags begins. This behavior is due to the reduction of the motor rotation, what basically demands a new startup and since the torque is low, the current with low power factor increases. When the voltage sag ends, this power produces a peak value of 0.5 pu due to the voltage recovery to 1 pu.

Figure V shows that, the behavior for active power for the three static model, did not present good performance, because they shown a slowly restoration during the disturbance from 0.82 to 0.85 pu. At the end of voltage sag, the active power goes slowly back to its initial value, taking around 30 cycles in comparison with the 10 cycles for the experimental result (Figure IV).

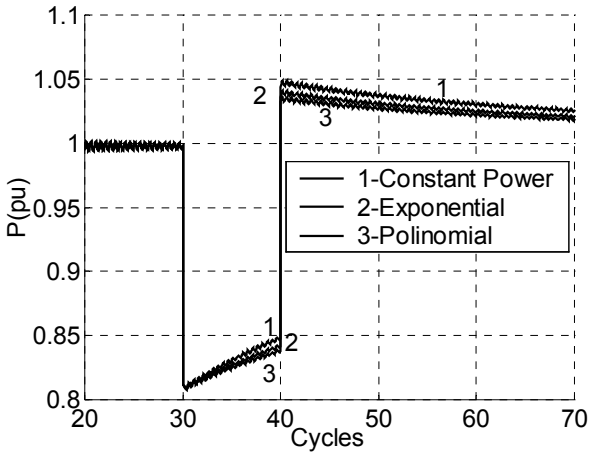

FIGURE V
Active power response for static models (case 1-simulation results)

Considering reactive power in the experimental results (Figure IV), the peaks at the beginning and at the end of disturbance were 0.35 pu, and 0.5 pu respectively, but Figure V shows that for the three static models the peak is 0.19 pu. Therefore these models are not able to represent air conditioner load.

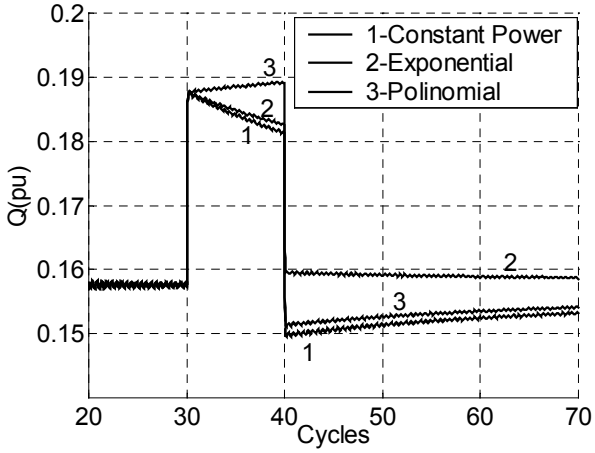

FIGURE VI
Reactive power response for static models (case 1-simulation results)

Figure VII shows the simulation results for the dynamic model where the active power presents greater peaks not only at the beginning but also at the end of the voltage sag. However, the reestablishment period is the same as that of the experimental test, i.e., around 10 cycles. The reactive power behavior is similar to that concerning the experimental tests, but the peak values are about 0.35 pu, and 0.3 pu, which are lesser than those obtained experimentally, i.e., 0.35 pu and 0.5 pu, respectively. Therefore the dynamic model proposed is more satisfactory than the static models.

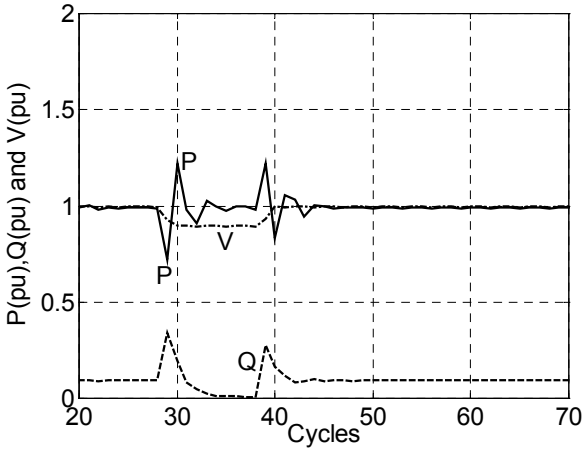

FIGURE VII
Voltage applied and active and reactive powers responses (case 1-simulation results)

V.II Case 2: 30% Voltage Sag during 05 cycles

Figure VIII shows a voltage sag applied to the air conditioner as well as the active power and reactive power responses. It can be seen that the active power decreases to 0.52 pu when the voltage sag begins and after that it seeks to be reestablished. When the voltage rises to 1.0 pu, the active power reaches a peak value equal to 1.85 pu and decreases to the nominal value after 10 cycles.

The reactive power assumes 0.6 pu and 0.95 pu at the beginning and at the end of the voltage sag, respectively. Such values are about three times the nominal value, i.e., 0.17 pu.

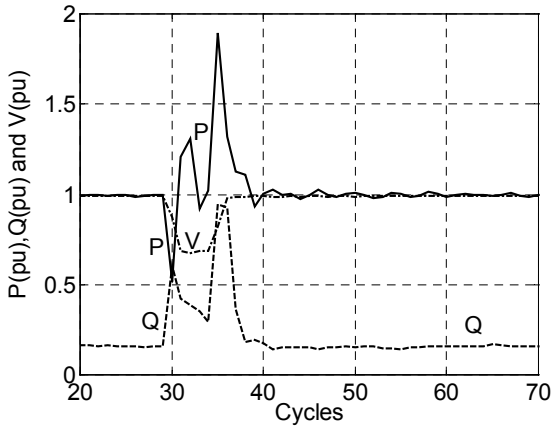

FIGURE VIII
Voltage applied and active and reactive powers responses (case 2 experimental results)

Figure IX and X show simulation results for static models, where the active and reactive power behaviors are practically the same for each static model. In this case it is possible to see that the responses are not similar to experimental results in both qualitative and quantitative forms, mainly during the disturbance.

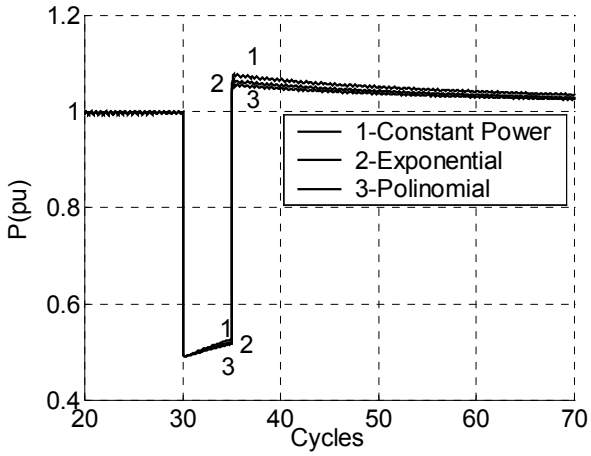

FIGURE IX
Active power responses for static models (case 2-simulation results)

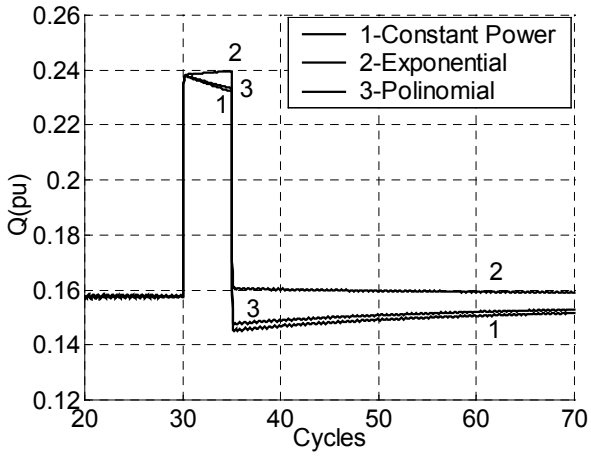

FIGURE X
Reactive power responses for static models (case 2-simulation results)

From the analysis of the dynamic model shown in Figure XI, it can be seen that the active power is reduced to 0.8 pu, while it assumes 0.59 pu in the experimental tests. When the supply voltage reestablishes the nominal value, the active power reaches 1.82 pu, not only experimentally but also in the simulation tests. The simulation results for the reactive power indicate greater values than those obtained experimentally not only at the beginning but also at the and of the disturbance, i.e., 0.9 pu and 1.2 pu, respectively, as the difference is equal to 0.3 pu. However, the nominal value obtained in the simulation is similar to the experimental one. The differences between the experimental and simulation results for the dynamic model are due to the presence of the fan motor, which was not included in the modeling.

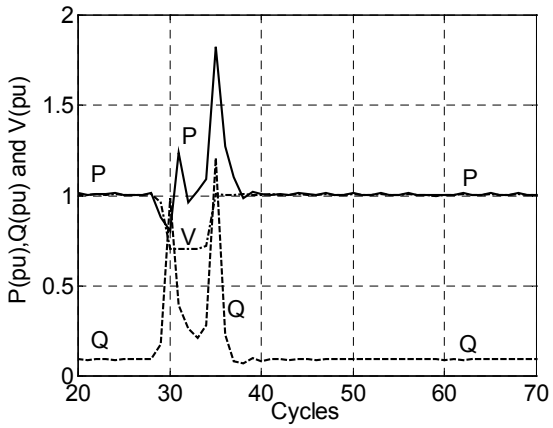

FIGURE XI
Voltage applied and active and reactive powers responses (case 2-simulation results)

V.III Case 3: Frequency variation between 57 and 63 Hz for voltages equal to 0.9, 1.0 and 1.1 pu

Frequency variations are other common phenomena that occurs in the power system mainly after faults, loss of generation or loss of load. In order to analyze the air conditioner performance under such disturbances, the voltage is fixed at three levels, i.e., 0.9 pu, 1.0 pu and 1.1 pu, as the frequency is varied from 57 Hz to 63 Hz (1 Hz step), by using a programmable power supply.

According to Figure XII, the curves regarding active power levels are practically not sensitive to the voltage, because the torque is directly proportional to the power transferred from the stator to the rotor, and it does not depend on the speed. However, it is obvious that this condition is not valid for lower voltage levels, since the rotor gets blocked. In this case the active power is more sensitive to the frequency variation, once the motor rotation is altered. The dynamic model has presented results similar to the experimental ones, implying that it is valid for the analysis of the active power behavior as a function of the frequency.

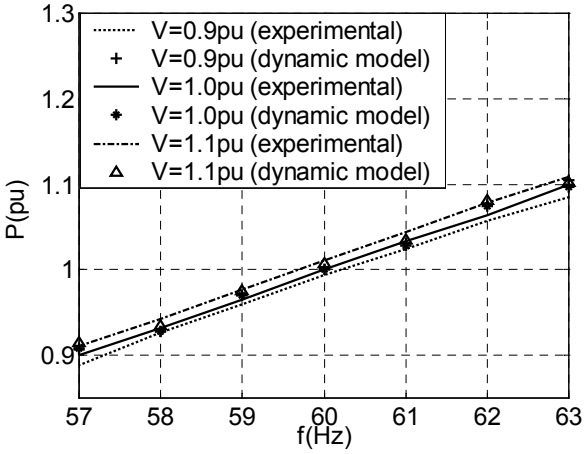

FIGURE XII
Active power versus frequency for three voltage levels (case 3)

On the other hand, Figure XIII shows that the reactive power is sensitive to both voltage and frequency, but the experimental results are greater than the simulated ones when the voltage is 0.9 pu. This can be explained once the fan has not been included in the dynamic model.

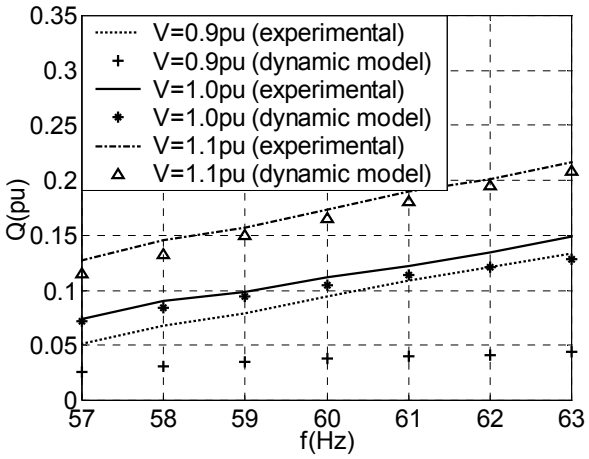

FIGURE XIII
Reactive power versus frequency for three voltage levels (case 3)

V. CONCLUSIONS

After simulation and experimental tests were carried out on the air conditioner, several significant results were obtained. At the beginning and at the end of voltage sags, there were high reactive power absorptions. They were approximately twice and three times the rated value for cases 1 and 2, respectively, mainly when the voltage was reestablished to its nominal value. Considering the simultaneous operation of several air conditioner loads, it may cause system overloads.

The traditional static models did not present good behavior for the disturbances applied, because they are formulated on algebraic approaches, without considering transient conditions.

The dynamic model performance was adequate to determine the active and reactive power responses when voltage sags occur, describing the system behavior accurately. As seen, the proposed model presented similar active power experimental and simulation results. On the other hand, it was seen that the reactive power results were quite different when the voltage is 0.9 pu, which can be explained by the lack of the representation of the air conditioner cooler fan.

ACKNOWLEDGEMENT

The authors acknowledge to CAPES by the financial support.

REFERENCES

[1] Del Toro, V. “Electromechanical Devices for Energy Conversion and Control Systems”. Englewood Cliffs, New Jersey, 1968. p. 384;

[2] Kurita , A.; Sakurai, T., “The Power System Failure on July 23, 1987 in Tokyo”. Proceedings of the 27th Conference on Decision and Control. Austin, Texas, p. 2093-2097, December 1988;

[3] Williams, B. R.; et al, “Transmission Voltage Recovery Delayed by Stalled Air Conditioner Compressors”. IEEE Transactions on Power Systems, IEEE, vol. 7, No. 3, p. 1173-1179, August 1992;

[4] Hain, Y. ; Schweitzer, I., “Analysis of the Power Blackout of June 8, 1995 in the Israel Electric Corporation”. IEEE Transactions on Power Systems, Vol. 12, No. 4, p. 1752-1758, November 1997;

[5] Souza, D.R., Guimarães, G.C., Oliveira, J.C., Moraes, A.J. “The use of simulator ‘SABER’ in voltage stability and collapse studies of electric power system”. VIII Symposium of Specialists in Electric Operational and Expansion Planning (VIII SEPOPE), Brasilia – DF, May 2002;

[6] Castillo, B. C.; Oliveira, J. C.; Delaiba, A. C., “Condicionador de Ar: Impacto da Qualidade da Energia de Suprimento no Desempenho do Equipamento”. Anais do XIV Congresso Brasileiro de Automática, p.335-340, Natal-RN, Setembro, 2002;

[7] SABER Reference Manual, Release 5.1, Analogy Inc., Beaverton, OR, 1999.